Oxidative decarboxylation of α-hydroxy acids by a functional model of the nonheme iron oxygenase, CloR†

Tapan Kanti Paine,*[a] Sayantan Paria[a] and Lawrence Que, Jr.*[b]

Received (in Berkeley, CA, USA) 2nd December 2009, Accepted 25th January 2010
First published as an Advance Article on the web 12th February 2010
DOI: 10.1039/b925389k

Iron(II)–α-hydroxy acid complexes of a tripodal N4 ligand undergo oxidative decarboxylation upon exposure to O_2 and mimic the aliphatic C1–C2 cleavage step catalyzed by CloR.

The large majority of nonheme iron enzymes that cleave C–C bonds are catechol dioxygenases, which take advantage of the electron-rich nature of the aromatic substrates to initiate O_2 activation.[1] There are now related enzymes that cleave aliphatic C–C bonds, but a different O_2 activation mechanism is required because of the difference in the substrates.[2] A recently characterized example is 2-hydroxyethylphosphonate (HEP) dioxygenase (HEPD) that catalyzes the cleavage of the HEP C1–C2 bond to form hydroxymethylphosphonate and formate.[2,3] The nonheme iron center is bound to a 2-His-1-carboxylate facial triad[4,5] and the substrate binds in a bidentate manner to the iron *via* the 2-OH and phosphonate groups.[3] Another example is CloR, an enzyme involved in the biosynthesis of clorobiocin,[6] an aminocoumarin antibiotic that targets bacterial DNA gyrase.[7,8] Clorobiocin has a 3DMA-4HB moiety (Scheme 1) that derives from 3DMA-4HPP *via* two consecutive oxidative decarboxylation steps catalyzed by CloR. Of interest to this work is the novel C1–C2 bond cleavage of 3DMA-4HMA in the second step. By analogy to HEPD, the mandelate substrate may bind in a bidentate fashion to the iron to initiate the O_2 activation mechanism. This notion is tested with model complexes in this study.

There are only two reports on the iron(II)–α-hydroxy-carboxylate complexes,[9,10] and no biomimetic iron(II) complexes that use O_2 for the selective oxidative decarboxylation of mandelic acid to benzoic acid. Thus, to develop an understanding of the reaction catalyzed by CloR, we have initiated the syntheses of a series of iron(II)–α-hydroxy acid complexes and associated reactivity studies. We report herein the structure of $[(6\text{-Me}_3\text{-TPA})\text{Fe}^{\text{II}}(\text{mandelate})]^+$ (**1**, 6-Me$_3$-TPA = tris-[(6-methyl-2-pyridyl)methyl]amine) and its reaction with dioxygen as well as those of other iron(II)–α-hydroxy acid complexes of the same tetradentate ligand.

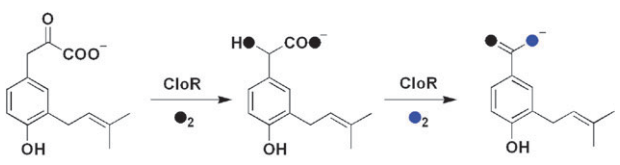

Scheme 1 Consecutive reactions catalyzed by bifunctional CloR.

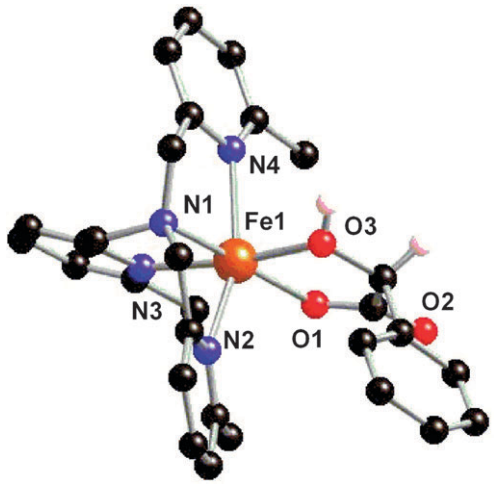

Fig. 1 Molecular structure of $[(6\text{-Me}_3\text{-TPA})\text{Fe}^{\text{II}}(\text{mandelate})]^+$ (**1**). All hydrogen atoms except those attached to O3 and the adjacent C23 atom have been omitted for clarity. Selected bond lengths [Å] and angles [°] for **1**: Fe1–O1 2.023(2), Fe1–O3 2.178(2), Fe1–N1 2.179(3), Fe1–N2 2.259(3), Fe1–N3 2.217(3), Fe1–N4 2.287(3), O1–C22 1.273(4), O2–C22 1.243(4), O3–C23 1.431(4); O1–Fe1–O3 76.40(8), O1–Fe1–N1 166.88(9), O1–Fe1–N3 111.96(9), O3–Fe1–N3 171.00(9).

The reaction of $Fe(ClO_4)_2\cdot 6H_2O$, 6-Me$_3$-TPA ligand, mandelic acid and triethylamine in methanol yields a light yellow iron(II) complex $[(6\text{-Me}_3\text{-TPA})\text{Fe}^{\text{II}}(\text{mandelate})]^+$ (**1**) with a monoanionic mandelate. The X-ray crystal structure of the monocationic complex **1** reveals a six-coordinate iron(II) center with a tetradentate tripodal ligand and a bidentate mandelate anion (Fig. 1). In the structure Fe1 has a distorted octahedral environment consisting of the tetradentate ligand and a bidentate mandelate anion coordinated *via* O1 and O3. The O3 oxygen is coordinated as hydroxy form and its hydrogen atom forms an intermolecular hydrogen bond with the noncoordinated carboxylate oxygen of a neighboring molecule. The Fe1–O1 bond distance of 2.023 Å is typical of an Fe(II)–carboxylate interaction, such as those found in the structures of $[(6\text{-Me}_3\text{-TPA})\text{Fe}^{\text{II}}(\text{benzoate})]^+$ (**2**) and $[(6\text{-Me}_3\text{-TPA})\text{Fe}^{\text{II}}(\text{benzoylformate})]^+$ (**3**),[11,12] and the C–O bond lengths of the carboxylate group of the coordinated

[a] *Department of Inorganic Chemistry, Indian Association for the Cultivation of Science, 2A&2B Raja S. C. Mullick Road, Jadavpur, Kolkata-700032, India. E-mail: ictkp@iacs.res.in; Fax: +91 33-2473-2805; Tel: +91 33-2473-4971*
[b] *Department of Chemistry and Center for Metals in Biocatalysis, University of Minnesota, 207 Pleasant Street SE, Minneapolis, MN 55455, USA. E-mail: larryque@umn.edu; Fax: +1 612-624-7029; Tel: +1 612-625-0389*

† Electronic supplementary information (ESI) available: Crystallographic data for **1** in CIF format, experimental and spectroscopic data. CCDC 701933. For ESI and crystallographic data in CIF or other electronic format see DOI: 10.1039/b925389k

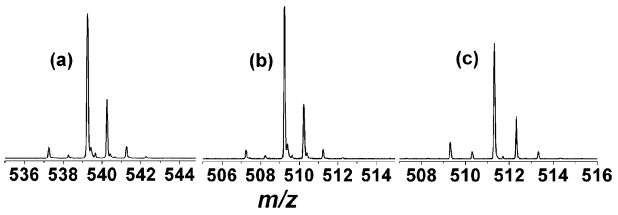

Fig. 2 ESI-MS (positive ion mode in MeCN) of (a) **1**, (b) the solution after oxidation of **1** with O_2 and (c) the solution after oxidation of **1** with $^{18}O_2$.

mandelate clearly indicate charge delocalization of the carboxylate. The longer Fe1–O3 distance of 2.178 Å is associated with the 2-OH ligand and consistent with a neutral hydroxyl oxygen comparable to the Fe–O distance found in $[(TPA)Fe^{II}(MeOH)_2]^{2+}$.[13] A shorter Fe–O bond distance (1.970 Å) for a negatively charged enolate oxygen is observed for an iron(II) complex with the same tripodal ligand.[14]

The ESI-MS spectrum of **1** in acetonitrile shows a dominant signal at m/z = 539.2 with the expected isotope distribution pattern indicating a monocationic complex with composition $[(6\text{-}Me_3\text{-}TPA)Fe^{II}(mandelate)]^+$ in solution (Fig. 2a). Complex **1** reacts with pure dioxygen in acetonitrile at ambient temperature over a period of 6 h. Monitoring the reaction by ESI-MS shows the time-dependent disappearance of the m/z = 539.2 peak concomitant with the appearance of a peak at m/z = 509.2 (Fig. 2b), with an isotope distribution pattern indicative of a mononuclear monocationic complex with an m/z value that matches that of $[(6\text{-}Me_3\text{-}TPA)Fe^{II}(benzoate)]^+$ (**2**).

The transformation of **1** to **2** can also be monitored by ^{1}H NMR. The α-CH_3 resonances of the 6-Me_3-TPA ligand in **1** appear as a broad paramagnetically shifted peak at −45 ppm due to the presence of four unpaired electrons on the high-spin iron(II) center (Fig. 3a). Upon exposure to O_2, the broad peak slowly diminishes in intensity and is replaced by a sharper resonance at −43 ppm (Fig. 3b–d). We associate this latter peak with the α-CH_3 resonances of independently prepared **2**[12] in CD_3CN but only after the addition of 1 equiv. H_2O. The

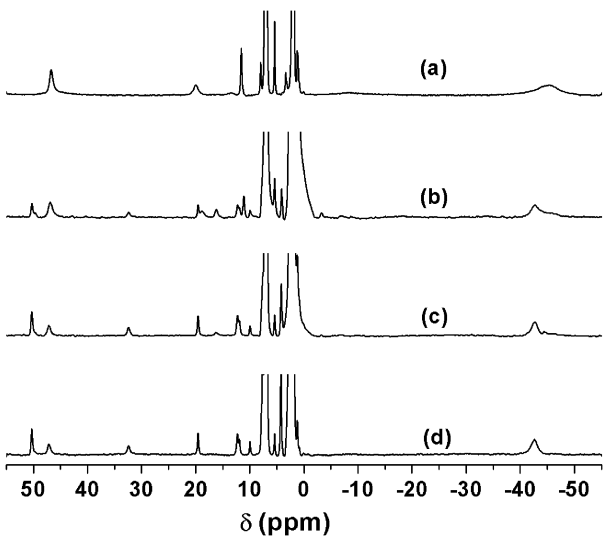

Fig. 3 ^{1}H NMR spectral changes of complex **1** in CD_3CN (a) during the reaction with O_2 at 25 °C after 2 h (b), 4 h (c) and 6 h (d) at 25 °C.

new features in the downfield region can also be associated with **2** in the presence of 1 equiv. H_2O. Extraction of the reaction solutions after acid treatment into organic solvent allows the mandelate-to-benzoate ratio to be determined; this method shows that mandelate is quantitatively converted to benzoate over the course of 6 h (Fig. S1, ESI†). Thus **1** converts to **2** upon exposure to O_2.

Iron(II) complexes of related α-hydroxy acids also undergo oxidative decarboxylation upon exposure to O_2. Replacement of the phenyl group with a methyl group affords $[(6\text{-}Me_3\text{-}TPA)Fe^{II}(lactate)]^+$ (**4**) that reacts with O_2 to form $[(6\text{-}Me_3\text{-}TPA)Fe^{II}(acetate)]^+$, but the reaction takes almost twice as long (10 h) as the reaction of **1**. The ESI-MS of the oxidized solution of **4** shows a peak at m/z = 447.2 which is 30 mass units less than the lactate complex indicative of the formation of the acetate complex (Fig. S2, ESI†). In addition the ^{1}H NMR peaks of the oxidized solution of **4** do match with those in independently synthesized acetate complex (Fig. S3, ESI†). The increase in the reaction time upon replacement of the mandelate α-CH bond with the stronger lactate α-CH bond suggests that the cleavage of the α-CH bond must partially contribute to the rate determining step.

The conversion of mandelate to benzoate is a $4e^-$-oxidation. To ascertain the incorporation of dioxygen in the oxidative decarboxylation reaction, the oxygenation reaction of **1** was carried out in an $^{18}O_2$ atmosphere in dry acetonitrile. The resulting benzoate product was analyzed by ESI-MS and this clearly showed the incorporation (>95%) of one ^{18}O atom into the carboxyl group of the product, as demonstrated by the molecular ion peak at m/z = 511.2 (Fig. 2c). The other ^{18}O atom involved in this step is most likely converted to water, which remains bound to the iron(II) center of the product and affects the chemical shift observed for the α-CH_3 resonances of the 6-Me_3-TPA ligand in **2**. Thus the conversion of **1** to **2** models the second oxidation reaction catalyzed by CloR.

Some insight into the mechanism of the oxidative decarboxylation of **1** can be gleaned from a comparison of the susceptibility of three $[Fe^{II}(6\text{-}Me_3\text{-}TPA)(X)]$ complexes to dioxygen, where X is mandelate (**1**), benzoate (**2**), and benzoylformate (**3**). Interestingly, **2** is air stable,[12] suggesting that the O_2 affinity of the iron(II) center is quite low. On the other hand, **3** reacted with O_2 over a period of 4 days resulting in the oxidative decarboxylation of the coordinated benzoylformate to give **2** in almost quantitative yield.[11] Complex **3** differs from **2** in having an α-keto group that binds to the iron(II) center. It seems unlikely that the introduction of this additional ligand would be sufficient to increase significantly the O_2 affinity of the iron(II) center in **3** relative to **2**. However what the α-keto group provides is an electrophilic carbonyl group to trap the nascent nucleophilic superoxide that forms upon O_2 binding to the iron(II) center, which drives the reaction forward and irreversibly towards oxidative decarboxylation. Remarkably, **1** reacted even faster with dioxygen, producing the same oxidatively decarboxylated product **2** over a period of only 6 h, a factor of 20-fold faster than **3**. The coordination of an alcohol as the sixth ligand in this complex, which is a better Lewis base than the corresponding carbonyl oxygens in **2** and **3**, may introduce sufficient electron density into the iron(II) center to increase its affinity for O_2. The nascent superoxide would then have to

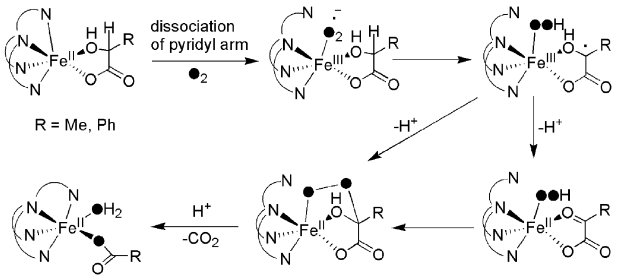

Scheme 2 Proposed mechanism for the oxidative decarboxylation of α-hydroxy acids.

initiate the oxidative decarboxylation reaction by abstracting the hydrogen atom from the α-CH bond of the substrate (Scheme 2). In support, we observed that the oxidative decarboxylation of **1** required 10 h for completion when mandelate-2-d_1 was used in place of mandelate, showing C–H bond cleavage is partially rate determining.

Further evidence for the crucial first step was obtained by the use of TEMPOH as an intercepting agent. Previously, TEMPOH was utilized effectively as a hydrogen atom donor by Karlin and co-workers to convert a structurally characterized copper(II)–superoxo complex to form a reactive copper(II)–hydroperoxo complex.[15] Thus, when **1** was oxygenated in the presence of 1 equiv. TEMPOH, TEMPO radical was produced in 8% yield relative to iron, as determined by integration of its characteristic $g = 2$ EPR signal (Fig. S4, ESI†). Furthermore NMR analysis of the organic products showed the presence of residual mandelate with a mandelate-to-benzoate ratio of 1 : 9 (Fig. S5, ESI†). Increasing the amount of added TEMPOH increased the amount of residual mandelate, changing the mandelate-to-benzoate ratio to 1 : 1 for 10 equiv. TEMPOH and 9 : 1 for 20 equiv. TEMPOH (Fig. S6, ESI†). The observed interception by TEMPOH suggests that the initially formed Fe–O_2 adduct has iron(III)–superoxide character and cleaves the weak O–H bond of TEMPOH in an intermolecular reaction that is in competition with intramolecular H-atom abstraction from the α-CH bond of mandelate.

In the C–C bond cleavage reaction catalyzed by HEPD, Whitteck and co-workers have proposed the abstraction of the C2–H atom from HEP by an iron(III)–superoxide species followed by hydroperoxylation and peroxo rearrangement to convert substrate into products.[2] On the basis of our experimental observations, we propose an analogous mechanism in Scheme 2 where the nascent superoxide abstracts the α-C–H atom of the α-hydroxyacid to initiate the oxidative decarboxylation reaction. In the next step, C–O bond formation between the α-carbon and the dioxygen-derived moiety occurs either by (a) coupling between the α-C$^{\bullet}$ radical and HOO$^{\bullet}$ or (b) electronic reorganization to generate an Fe^{II}(OOH)(α-ketoacid) complex followed by nucleophilic attack of HOO^{-} on the α-keto group. In either pathway, the resulting peroxy adduct would then spontaneously undergo oxidative decarboxylation.

In summary, we have characterized two iron(II) complexes of α-hydroxy acids that undergo oxidative decarboxylation upon exposure to O_2. An iron(III)–superoxo species is implicated in the reaction mechanism. These model complexes thus serve as functional mimics of the nonheme iron enzyme CloR and, by extension, HEPD, both of which oxidatively cleave aliphatic C–C bonds and highlight the versatility of nonheme iron in catalyzing various oxidations in biology.

This work was supported by the U.S. National Institutes of Health (GM-33162 to L.Q.) and the DST, India (Project SR/S1/IC-10/2006 to T.K.P.). S.P. thanks CSIR, India, for a fellowship. We thank Dr Victor G. Young, Jr., William W. Brennessel, and Benjamin Kucera of the University of Minnesota X-ray Crystallographic Laboratory for determining the crystal structure of **1**.

Notes and references

1 J. D. Lipscomb and A. M. Orville, in *Metal Ions in Biological Systems*, ed. H. Sigel and A. Sigel, Marcel Dekker, New York, 1992, vol. 28, pp. 243–298.
2 J. T. Whitteck, R. M. Cicchillo and W. A. van der Donk, *J. Am. Chem. Soc.*, 2009, **131**, 16225–16232.
3 R. M. Cicchillo, H. Zhang, J. A. V. Blodgett, J. T. Whitteck, G. Li, S. K. Nair, W. A. van der Donk and W. W. Metcalf, *Nature*, 2009, **459**, 871–874.
4 E. L. Hegg and L. Que, Jr., *Eur. J. Biochem.*, 1997, **250**, 625–629.
5 K. D. Koehntop, J. P. Emerson and L. Que, Jr., *J. Biol. Inorg. Chem.*, 2005, **10**, 87–93.
6 F. Pojer, R. Kahlich, B. Kammerer, S.-M. Li and L. Heide, *J. Biol. Chem.*, 2003, **278**, 30661–30668.
7 S. C. Kampranis, N. A. Gormley, R. Tranter, G. Orphanides and A. Maxwell, *Biochemistry*, 1999, **38**, 1967–1976.
8 A. Maxwell and D. M. Lawson, *Curr. Top. Med. Chem.*, 2003, **3**, 283–303.
9 R. Carballo, B. Covelo, E. M. Vázquez-López, E. García-Martínez, A. Castiñeiras and C. Janiak, *Z. Anorg. Allg. Chem.*, 2005, **631**, 2006–2010.
10 A. Beghidja, G. Rogez, P. Rabu, R. Welter and M. Drillon, *J. Mater. Chem.*, 2006, **16**, 2715–2728.
11 Y.-M. Chiou and L. Que, Jr., *J. Am. Chem. Soc.*, 1995, **117**, 3999–4013.
12 J. Kim, Y. Zang, M. Costas, R. G. Harrison, E. C. Wilkinson and L. Que, Jr., *J. Biol. Inorg. Chem.*, 2001, **6**, 275–284.
13 A. Diebold and K. S. Hagen, *Inorg. Chem.*, 1998, **37**, 215–223.
14 T. K. Paine, H. Zheng and L. Que, Jr., *Inorg. Chem.*, 2005, **44**, 474–476.
15 D. Maiti, D.-H. Lee, K. Gaoutchenova, C. Würtele, M. C. Holthausen, A. A. N. Sarjeant, J. Sundermeyer, S. Schindler and K. D. Karlin, *Angew. Chem., Int. Ed.*, 2008, **47**, 82–85.

